

AperTO - Archivio Istituzionale Open Access dell'Università di Torino

The Importance of Interactions at the Molecular Level: A Spectroscopic Study of a New Composite Sorber Material

This is the author's manuscript

Original Citation:

Availability:

This version is available <http://hdl.handle.net/2318/1652806> since 2017-11-23T12:19:21Z

Published version:

DOI:10.1177/0003702817723053

Terms of use:

Open Access

Anyone can freely access the full text of works made available as "Open Access". Works made available under a Creative Commons license can be used according to the terms and conditions of said license. Use of all other works requires consent of the right holder (author or publisher) if not exempted from copyright protection by the applicable law.

(Article begins on next page)



UNIVERSITÀ DEGLI STUDI DI TORINO

This is an author version of the contribution published on:

Questa è la versione dell'autore dell'opera:

The importance of the interactions at the molecular level:
spectroscopy study of a new composite sorber material

by

*Valentina Crocellà, Elena Groppo, Alessandro Dani, Alberto Castellero, Silvia Bordiga,
Stefano Zilio, Agnello De Simone and Paolo Vacca*

Applied Spectroscopy, 2017, 71, 2278-2285

DOI 10.1177/0003702817723053

The definitive version is available at:

La versione definitiva è disponibile alla URL:

<http://journals.sagepub.com/doi/abs/10.1177/0003702817723053?journalCode=aspc>

The importance of interactions at the molecular level: spectroscopic study of a new composite sorber material

Valentina Crocellà¹, Elena Groppo¹, Alessandro Dani¹, Alberto Castellero¹, Silvia Bordiga¹,
Stefano Zilio², Agnello De Simone² and Paolo Vacca^{2,*}

¹ Dipartimento di Chimica, NIS and INSTM Centre of Reference, Università di Torino, Via Quarello 15/A,
10135 Torino (Italy)

² SAES Getters S.p.A., Viale Italia 77, 20020 Lainate, Italy

*Corresponding author: P. Vacca. E-mail address: Paolo_Vacca@saes-group.com)

Abstract

The functional properties of a new composite material having water vapor getter properties have been investigated by a large arsenal of characterization techniques. The composite system is originated by combining two constituents having very different chemical natures, a $\text{Mg}(\text{ClO}_4)_2$ salt and a polymeric acrylic matrix. In particular, FT-IR and Raman spectroscopy has been fundamental to understand the type of interactions between the salt and the matrix in different hydration conditions. It was found that in the anhydrous composite system the dispersed $\text{Mg}(\text{ClO}_4)_2$ salt retains its molecular structure, because Mg^{2+} cations are still surrounded by their $[\text{ClO}_4]^-$ counter-anions; at the same time the salt and the polymeric matrix chemically interact each other at the molecular level. These interactions gradually vanish in the presence of water, up to disappear in the

fully hydrated composite system, where the Mg^{2+} cations are completely solvated by the water molecules.

Keywords: solid state drier, composite, magnesium perchlorate, in situ spectroscopic techniques, polymeric matrix.

1. Introduction

Moisture is a harmful contaminant for many electronic and opto-electronic devices, reducing their lifetime even at low concentration levels (<0.5% vol).^{1,2} This effect is particularly dangerous for organic semiconductors with large band gap energy.³ The most common way to remove moisture is to include a proper getter in the device. Beside a good moisture adsorption rate and capacity, a suitable getter must possess other important features such as high transmittance in the visible light range. Composite materials based on an active getter compound dispersed in organic matrices possesses the ideal properties to be employed as getters in different types of device. Among the possible active getter phases, hygroscopic salts exhibit a very high moisture adsorption rate, provided that they are finely dispersed, or possibly dissolved at a molecular level. To achieve this goal, the salt must interact with the matrix. It is thus clear that the composite material having the best getter properties may be optimized by selecting the right couple of salt and matrix so that their reciprocal interaction is beneficial for achieving a good dispersion and simultaneously allowing an optimum interaction with water. A rational design of such a composite material requires a thorough characterization of the properties of both the salt and the matrix, before investigating the composite itself.

In the present paper, we report on the properties of a model composite system based on $\text{Mg}(\text{ClO}_4)_2$ salt dispersed in a polymeric acrylic matrix. The combination of two constituents having

very different chemical natures gives rise to a composite system having unprecedented drying ability. In order to understand the reasons for these exceptional properties we have undertaken, at first, a thorough characterization of the salt as a function of its hydration conditions by means of a large arsenal of characterization techniques, among which in situ XRPD measurements, TGA, FT-IR (in both Mid and Far regions) and Raman spectroscopy. Vibrational techniques reveal to be very sensitive to the symmetry of the $\text{Mg}(\text{ClO}_4)_2$ salt at a molecular level and therefore they have been employed in a second step to investigate the properties of the composite material, with the aim to understand in which way the salt and the matrix interact each other and which is the behavior of the material in the presence of water. It is worth noting that Far-IR measurements are the only ones that give access to the $\nu(\text{Mg-O})$ vibrational region, and are fundamental to discriminate between hydrated and anhydrous forms of highly dispersed $\text{Mg}(\text{ClO}_4)_2$ salt. The final goal is to demonstrate that chemical interactions at a molecular level are fundamental in determining the functional properties of this composite material.

2. Experimental

2.1 Materials

The composite material (hereafter referred to as SSD, standing for *Solid Solution Dryer*) consists of a dehydrated perchlorate salt [$\text{Mg}(\text{ClO}_4)_2$] dispersed in a glycol-acrylate polymeric matrix (10 % wt) and was synthesized as described in detail elsewhere.⁴ Briefly, the salt was dissolved in the organic matrix, the solution was spread out using doctor blade or analogous techniques and then the polymerization process was triggered: a self-standing transparent film was thus obtained.

Pure $\text{Mg}(\text{ClO}_4)_2$ (for spectroscopic analysis), $\text{Mg}(\text{ClO}_4)_2 \cdot 6\text{H}_2\text{O}$, and pure glycol-acrylate matrices were purchased by Sigma-Aldrich (reagent grade), and used as received without purification.

Dehydrated $\text{Mg}(\text{ClO}_4)_2$ to be mixed with the organic matrix to get SSD was prepared from the $\text{Mg}(\text{ClO}_4)_2 \cdot 6\text{H}_2\text{O}$ salt by heating under vacuum using a proprietary process.

2.2 Techniques

X-Ray Powder Diffraction (XRPD). XRPD measurements were performed by means of a PW3050/60 X'Pert PRO MPD diffractometer from PANalytical, using as source the high power ceramic tube PW3373/10 LFF with a Cu anode equipped with Ni filter to attenuate $\text{K}\beta$. Scattered photons were collected by a RTMS (Real Time Multiple Strip) X'celerator detector. The SSD sample was measured in the flat configuration, whereas the anhydrous $\text{Mg}(\text{ClO}_4)_2$ salt was measured in a capillary filled in the glove-box and sealed under nitrogen atmosphere. In-situ XRPD measurements at different temperatures were performed using a PANalytical X'Pert diffractometer (Cu $\text{K}\alpha$ radiation) and inserting the sample into an Anton Paar XRK 900 reactor chamber equipped with a hot stage. A sequence of isothermal measurements were performed every 10 °C between 25 °C and 165 °C: the heating rate between each isotherm was 2 °C/min.

Termogravimetric analysis (TGA) and Differential scanning calorimetry (DSC). TGA and DSC measurements were performed under N_2 flow (heating ramp 2 °C/min) by means of a TA Q600 analyzer and a TA Q200 analyzer, respectively.

Raman spectroscopy. Raman spectra were recorded by using a Renishaw Raman Microscope spectrometer. An Ar^+ laser emitting at 514 nm was used as exciting source, in which the output power was limited to 50% (100% power = 2 mW at the sample) in order to avoid sample damage. The photons scattered by the sample were dispersed by a 1800 lines/mm grating monochromator and simultaneously collected on a CCD camera; the collection optic was set at 20x objective. The spectra were obtained by collecting 50 acquisitions (each of 10 s). All samples were measured inside a homemade cell equipped with a suprasil quartz cuvette that allowed measurements in controlled atmosphere to be performed. Pure $\text{Mg}(\text{ClO}_4)_2$ and $\text{Mg}(\text{ClO}_4)_2 \cdot 6\text{H}_2\text{O}$ were measured in the form of self-supporting pellets. The SSD composite and the corresponding matrix were measured in

the form of self-standing films in both dehydrated and hydrated conditions. To reach these two different dehydration stages, the samples were first degassed at room temperature overnight into the Raman cell, and then contacted directly with water vapor ($p_{\text{eq}} = 11$ mbar).

FT-IR spectroscopy. FT-IR spectra have been acquired with three different experimental set-up:

- 1) FT-IR spectra of $\text{Mg}(\text{ClO}_4)_2$ and $\text{Mg}(\text{ClO}_4)_2 \cdot 6\text{H}_2\text{O}$ in the mid-infrared spectral region were collected in ATR mode directly inside the glove-box, so avoiding the contact of these two salts with the atmosphere, by means of a Bruker Alpha instrument equipped with a diamond crystal. The ATR spectra are shown in ATR mode, i.e. after correction for the energy dependence of the penetration depth. This means that the ATR spectra are perfectly comparable with the transmission ones.
- 2) FT-IR spectra of SSD and of its matrix were collected in transmission mode in the mid-infrared spectral region at 2 cm^{-1} resolution on a Bruker Vertex 70 spectrophotometer equipped with a DTGS detector. Transmission mode has been selected in order to achieve enough sensitivity in the spectral regions where the interactions at molecular level mainly contribute. The samples were examined in the form of self-standing films placed inside a home-made quartz cell, equipped with KBr windows, connected to a conventional high-vacuum line (UHV) that allows samples activation and spectra acquisition in strictly *in situ* conditions. The materials were at first degassed at room temperature overnight and then contacted with increasing amount of water vapor.
- 3) Far-infrared spectra were recorded at 2 cm^{-1} resolution on the same Bruker Vertex 70 instrument equipped with a Si beam splitter and a DTGS detector for Far-IR region. $\text{Mg}(\text{ClO}_4)_2$ and $\text{Mg}(\text{ClO}_4)_2 \cdot 6\text{H}_2\text{O}$ were measured in the form of self-supporting pellets prepared by mixing the powder with a proper amount of paraffin wax (transparent to IR radiation in the $400\text{-}100\text{ cm}^{-1}$ range). Paraffin has the additional advantage to protect the sample from H_2O contamination, at least for some minutes. SSD and its matrix were measured as self-standing films. All the films were previously degassed overnight at room temperature in order to remove most of the

physisorbed water, and then quickly positioned inside the instrument chamber, which is fluxed with dry-air. After degassing the material at room temperature overnight, a series of spectra were collected at different time of exposure with the atmosphere.

3. Results and Discussion

3.1 Properties of $\text{Mg}(\text{ClO}_4)_2$ salt in different hydration states.

The $\text{Mg}(\text{ClO}_4)_2 \cdot 6\text{H}_2\text{O}$ salt dehydrates in two main steps, yielding consecutively the di-hydrate and anhydrate phases, as determined by TGA analysis (Figure 1a). In particular, four H_2O molecules are lost gradually in the 60-160 °C range to give the $\text{Mg}(\text{ClO}_4)_2 \cdot 2\text{H}_2\text{O}$ phase, through the tetrahydrate intermediate (peak at 105 °C in the derivative signal). The following conversion of $\text{Mg}(\text{ClO}_4)_2 \cdot 2\text{H}_2\text{O}$ into anhydrous $\text{Mg}(\text{ClO}_4)_2$ occurs in the 160-230 °C range: this last step is accompanied by the melting of the salt, as demonstrated by DSC data (endothermic peak around 150 °C, Figure 1b).

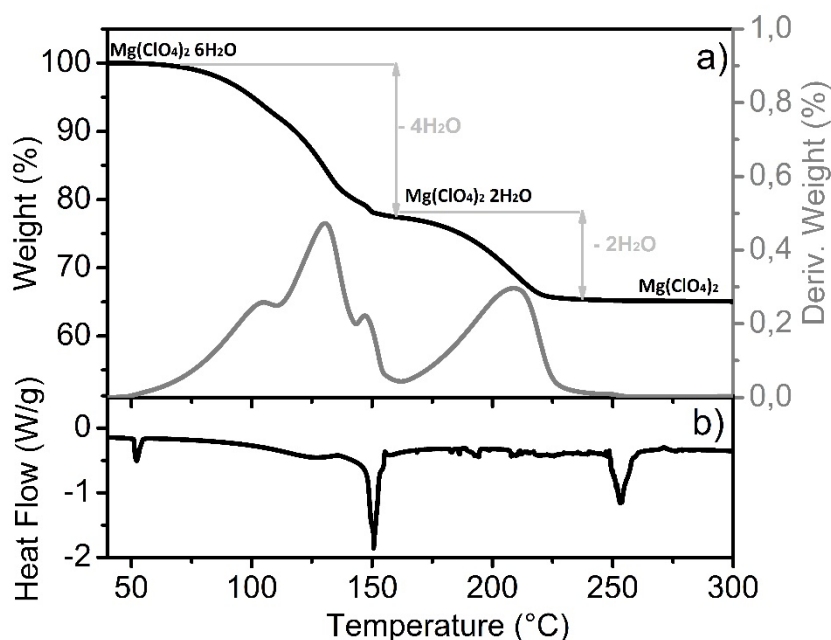


Figure 1. Weight loss (%) and its derivative signal (part a) and DSC signal (part b) as obtained from TGA and DSC measurements on $\text{Mg}(\text{ClO}_4)_2 \cdot 6\text{H}_2\text{O}$ heated from 25 to 300 °C at a rate of 2 °C/min in N_2 atmosphere.

The water loss involves a structural rearrangement and a decrease in symmetry: three different stable phases were identified, having six, four and two H₂O molecules and possessing a distinct X-ray diffraction pattern.⁵ For these three phases, a schematic representation of the central units around the Mg²⁺ cations is reported in Figure 2a-c. In Mg(ClO₄)₂·6H₂O (Figure 2a) the Mg²⁺ cation is surrounded by six water molecules in a very symmetric environment. The symmetry is lowered in the two intermediate phases (Figure 2b,c), where the Mg²⁺ cation is surrounded by four (two) water molecules and two (four) [ClO₄]⁻ anions. In anhydrous Mg(ClO₄)₂ (Figure 2d) the central unit is again highly symmetric, being the Mg²⁺ cation surrounded by six [ClO₄]⁻ anions. In particular, the structure of anhydrous Mg(ClO₄)₂ consists of MgO₆ octahedra and ClO₄ tetrahedra connected one to each other by corner-sharing. Each ClO₄ tetrahedron shares corners with three MgO₆ octahedra; the ClO₄ tetrahedron also has one dangling O atom, and can be classified as a bridging tridentate anion.⁶

The dehydration of the Mg(ClO₄)₂·6H₂O salt was followed by means of *in situ* XRPD measurements performed at increasing temperature up to 160 °C.

Figure 2 reports the whole set of patterns, whereas a detailed analysis of three selected patterns collected at three significant temperatures is reported in Figure S2 of the supporting information. At 35 °C, the experimental pattern (dark grey) coincides with that of hexahydrate Mg(ClO₄)₂. Above 80 °C the Mg(ClO₄)₂·6H₂O phase progressively disappears in favor of the Mg(ClO₄)₂·4H₂O phase. This phenomenon is maximized at 105 °C, when the experimental pattern (pink) shows a series of reflections consistent with the co-presence of both Mg(ClO₄)₂·4H₂O and a residual fraction of Mg(ClO₄)₂·6H₂O. The transient tetrahydrate phase quickly dehydrates to the Mg(ClO₄)₂·2H₂O phase. At 145 °C the XRPD pattern (violet) contains reflections due to Mg(ClO₄)₂·2H₂O together with signals of residual Mg(ClO₄)₂·4H₂O and Mg(ClO₄)₂·6H₂O. Above 145 °C all the reflections gradually disappear due to the gradual melting of the salt,⁷ in agreement with DSC data (Figure 1b). Fully dehydrated perchlorate can be obtained only upon melting the hexahydrate salt at 250 °C and subsequently cooling the product in totally anhydrous conditions.^{6,8}

In a second moment, we investigated the vibrational properties of both anhydrous and hexahydrate $\text{Mg}(\text{ClO}_4)_2$ salts by means of Raman and FT-IR spectroscopy.

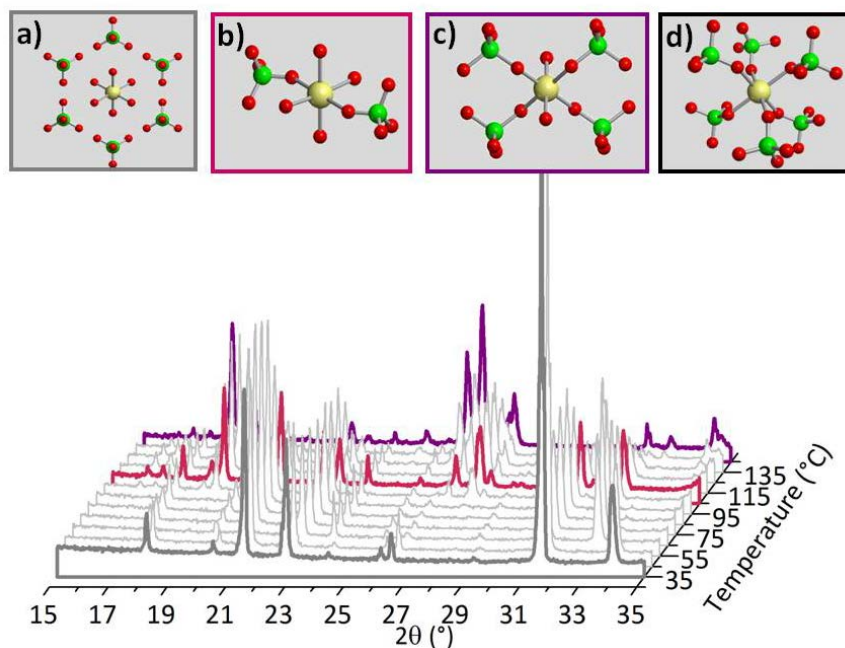


Figure 2. XRPD patterns collected during progressive heating of the hexa-hydrate $\text{Mg}(\text{ClO}_4)_2$ salt at increasing temperatures from 30 to 160 °C with a ramp of 2 °C/min. The patterns in bold correspond to three significant temperature steps at which $\text{Mg}(\text{ClO}_4)_2 \cdot 6\text{H}_2\text{O}$ (grey), $\text{Mg}(\text{ClO}_4)_2 \cdot 4\text{H}_2\text{O}$ (pink) and $\text{Mg}(\text{ClO}_4)_2 \cdot 2\text{H}_2\text{O}$ (violet) prevail. Insets show a schematic representation of the central units around the Mg^{2+} cations in four different hydration steps (Mg: light yellow; O: red; Cl: green).

Both FT-IR and Raman spectra of the hexahydrate $\text{Mg}(\text{ClO}_4)_2$ salt (grey spectra in Figure 3) are quite simple. Three highly symmetric bands are evident in the Raman spectrum (Figure 3a) at 934, 630 and 460 cm^{-1} , which are easily ascribed to the ν_1 (symmetric stretching, non-degenerate), ν_4 (asymmetric bending, triply degenerate) and ν_2 (symmetric bending double degenerate) Raman active modes of the $[\text{ClO}_4]^-$ group in perfect T_d symmetry.⁹⁻¹⁴ The IR active ν_3 vibrational mode (asymmetric stretching, triply degenerate) is observed in the FT-IR spectrum at 1052 cm^{-1} (Figure 3b).⁹⁻¹⁴ No signals are evident in the Raman spectrum below 400 cm^{-1} , while two absorption bands are observed in the far-IR spectrum at 200 and 120 cm^{-1} , overlapped to a rising background due to

the presence of water. These bands are ascribed to the Mg-O vibrations, where oxygen belongs to the six water molecules surrounding the magnesium cations (Mg-O_{H₂O}) and not to the oxygens of the [ClO₄]⁻ groups. However, the only comparable experimental data available in the literature is the far-IR spectrum of a Mg(ClO₄)₂ solution in water that exhibits well defined bands (after subtraction of the bulk water spectrum) at 421 and 178 cm⁻¹,¹⁵⁻¹⁶ i.e. at definitely higher wavenumbers with respect to our experimental results in the same spectral range. This difference could be explained considering that when the Mg(ClO₄)₂ salt is dissolved in H₂O, the solvation effect, which is not present in the solid state, might considerably affect its vibrational features. The presence of the two bands at 200 and 120 cm⁻¹ in the far-IR region of the hexahydrate salt and the Raman spectral profile of the [ClO₄]⁻ anions, provide an evidence that in Mg(ClO₄)₂·6H₂O water molecules solvate the Mg²⁺ cations, making the [ClO₄]⁻ groups highly symmetric. ^{10,15}

The Raman and FT-IR spectra of anhydrous Mg(ClO₄)₂ (black spectra in Figure 3) are much more complex. Each fundamental vibrational mode of the [ClO₄]⁻ group is split in at least two bands. This observation is consistent with the reduction of the symmetry for the [ClO₄]⁻ group, due to a partial covalent bonding between one or more of its oxygen atoms and the Mg²⁺ cation.¹⁴ In particular, the Raman spectrum (Figure 3a) exhibits four double bands centered at 1045 cm⁻¹ (ν₃), 970 cm⁻¹ (ν₁), 630 cm⁻¹ (ν₄) and 465 cm⁻¹ (ν₂). Two predominant complex absorptions, are evident in the FT-IR spectrum (Figure 3b) around 1160 and 640 cm⁻¹, which are ascribable to the IR active ν₃ and ν₄ vibrations, respectively.

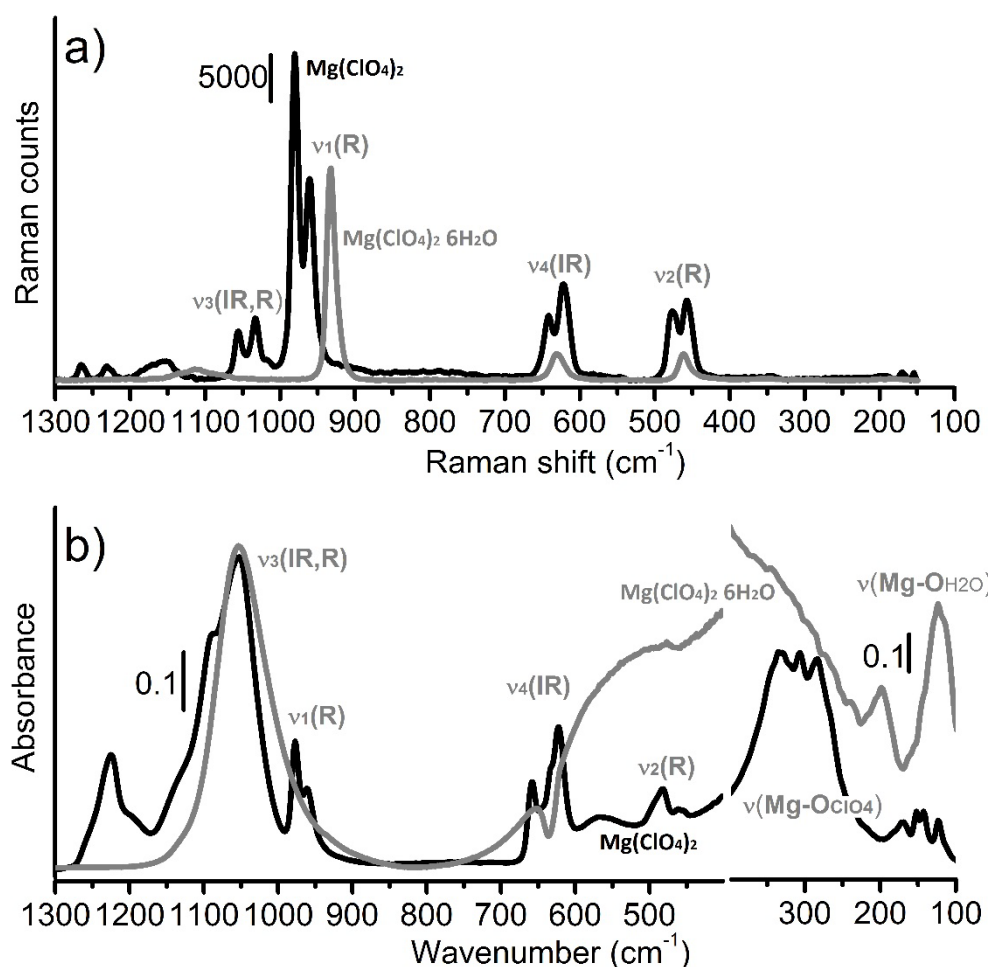


Figure 3. Raman ($\lambda = 514$ nm, part a) and FT-IR (part b) spectra of $\text{Mg}(\text{ClO}_4)_2$ in both anhydrous (black) and hexahydrate (grey) forms. Infrared and Raman active modes are labeled with (IR) and (R) respectively.

The FT-IR spectrum exhibits also two band envelopes at around 965 and 470 cm^{-1} due to the Raman active ν_1 and ν_2 modes.¹¹ The observation in the IR spectrum of absorption bands due to Raman active vibrations further confirms the perturbation of the $[\text{ClO}_4]^-$ groups induced by the coordination with the Mg^{2+} cations. Similar complex spectra in the mid-IR region are shown by other perchlorate salts (see Figure S2 of the supporting information), especially when the metal- ClO_4^- bond exhibits a high covalent character and the cation is big and divalent (such as $\text{Ba}(\text{ClO}_4)_2$ and $\text{Sr}(\text{ClO}_4)_2$). In the Far-IR region, the spectrum of anhydrous salt is dominated by a complex envelope of bands in the 390 - 200 cm^{-1} range. Considering that $\text{Mg}(\text{ClO}_4)_2$ is classified as a covalent perchlorate (in which the $[\text{ClO}_4]^-$ anion is covalently bonded to the Mg^{2+} cation),¹⁴ and that Pascal

et al. ascribe the absorption bands at around 250 cm^{-1} in the spectra of the isostructural Ni and Co perchlorates to the metal-oxygen stretching,¹³ we assign the set of bands centered at around 300 cm^{-1} (maxima at 331 , 307 and 285 cm^{-1}) to Mg-O_{ClO₄} vibrations. The weaker bands in the 200 - 100 cm^{-1} region are tentatively ascribed to collective vibrations involving relative movement of the cations and the anions.

3.2 The salt-matrix composite system in the anhydrous form.

The salt-matrix composite system (SSD) results from the combination of the anhydrous Mg(ClO₄)₂ salt with the polymeric matrix. Hence, it might be expected that its properties derive from the combination of the properties of the two constituents. This is not the case, and it is the key to understand the functional properties of the SSD. Starting from the structural properties, the XRPD pattern of the SSD in its anhydrous form (Figure S4) does not show any peak related to the Mg(ClO₄)₂ salt, but only a broad halo centered around $2\theta = 20^\circ$, which is due to the amorphous polymeric matrix. These data demonstrate that anhydrous Mg(ClO₄)₂ is highly dispersed into the matrix.

Figure 4 reports the FT-IR (parts a and c) and Raman (part b) spectra of the dehydrated SSD (red) in the most informative wavenumbers region. Both of them are not the pure sum of the spectra of the two starting components, i.e. plain matrix (light grey) and anhydrous Mg(ClO₄)₂ salt (black). The Raman spectrum of SSD (Figure 4b) is dominated by sharp absorption bands characteristic of the [ClO₄]⁻ vibrations, overlapped to broad and weak signals due to vibrations involving the amorphous polymeric matrix. The sharp absorption bands assigned to the [ClO₄]⁻ groups are larger in number and downward shifted with respect to the pure anhydrous Mg(ClO₄)₂ salt, and their intensity ratio is greatly modified. The complexity of the Raman spectrum suggests that the [ClO₄]⁻ groups in SSD are characterized by an even lower symmetry than in the anhydrous salt, which in turns means that the polymeric matrix does not play a simple solvation role.

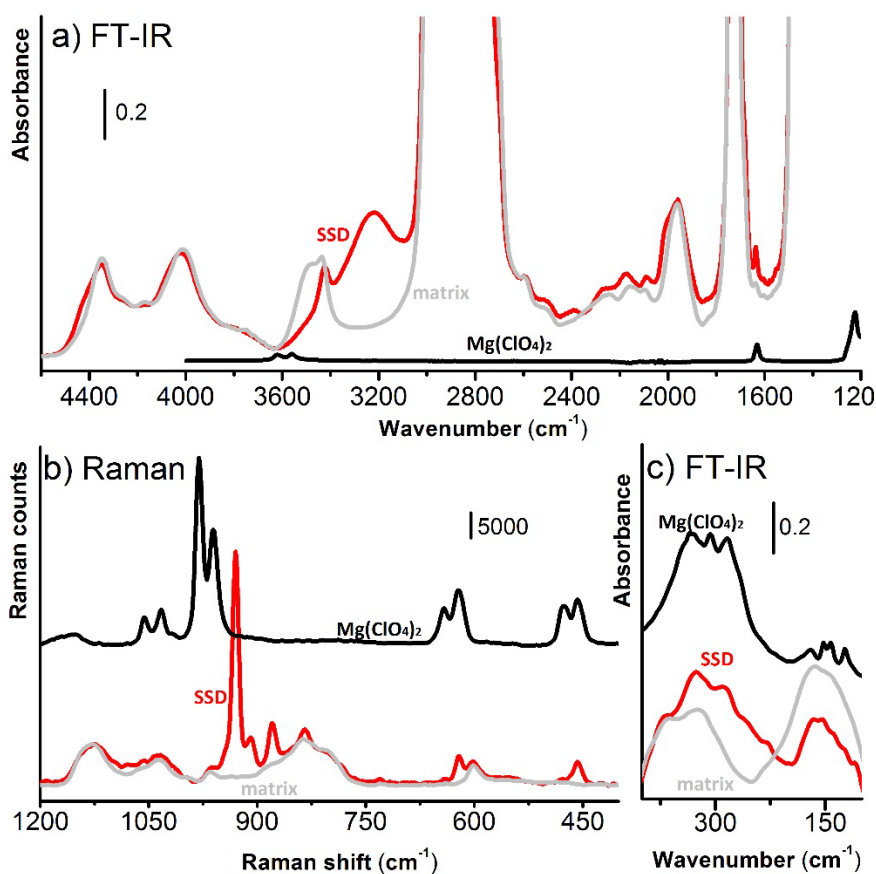


Figure 4. FT-IR (parts a and c) and Raman ($\lambda = 514$ nm, part b) spectra of anhydrous $\text{Mg}(\text{ClO}_4)_2$ (black, vertically translated), of the polymeric matrix (light grey) and of dehydrated SSD (red).

On the contrary, the FT-IR spectrum of SSD is dominated by the absorption bands of the polymeric matrix (Figure 4a and c), most of them out-of-scale and hence scarcely informative. However, some relevant differences are observed with respect to the spectrum of the pure matrix, especially in the Far-IR region (Figure 4c). In this range the spectrum of the matrix is dominated by two broad absorption bands around 350 and 160 cm^{-1} . Besides these bands, the spectrum of SSD shows an additional set of bands centered around 300 cm^{-1} , which are very similar to those observed in the spectrum of anhydrous $\text{Mg}(\text{ClO}_4)_2$ salt, and therefore are ascribed to $\text{Mg}-\text{O}_{\text{ClO}_4}$ stretching vibrations. This observation provides an evidence that the $[\text{ClO}_4]^{2-}$ groups are still in interaction with the Mg^{2+} cations in dehydrated SSD. Smaller differences between the spectra of SSD and that of the pure matrix are observed in the high wavenumbers region (Figure 4a). The most relevant difference concerns the IR band at 4345 cm^{-1} , ascribable to some combination of vibrational modes of the

matrix. In the FT-IR spectrum of SSD an additional shoulder is visible at 4430 cm^{-1} , which demonstrates that the matrix is perturbed by the presence of the salt. Finally, although dehydrated, SSD contains a very small amount of water (weak and broad absorption band at around 3220 cm^{-1} and weak signal at around 1636 cm^{-1} , ascribable to the ν_{OH} stretching and δ_{HOH} bending modes of water), absent in the spectrum of the plain matrix, and likely associated to the presence of a few defective sites to which a small fraction of water remains irreversibly adsorbed.

The whole set of results discussed above clearly demonstrate that in anhydrous SSD the $\text{Mg}(\text{ClO}_4)_2$ salt is highly dispersed and retains its “molecular structure”, meaning that the Mg^{2+} cations are still surrounded by their $[\text{ClO}_4]^{2-}$ counter-anions. This is directly proved by the observation of absorption bands due to $\text{Mg}-\text{O}_{\text{ClO}_4}$ stretching modes in the Far-IR spectrum. Nevertheless, the dispersed $\text{Mg}(\text{ClO}_4)_2$ salt feels the presence of the polymeric matrix, as demonstrated by the vibrational manifestations of the $[\text{ClO}_4]^{2-}$ groups in the Raman spectrum (which are indicative of a strong distortion from the T_d symmetry). Hence, in anhydrous SSD the two constituents interact each other at the molecular level.

3.3 Interaction of SSD with H_2O .

Before evaluating the behavior of the composite material in hydrated conditions, the interaction of the pure matrix with water was considered. The FT-IR spectra, in the mid-IR region, of dehydrated matrix (orange spectrum) and of the matrix after the contact with increasing pressures of water vapors (thin grey and blue spectra) were reported in Figure S5 of the supporting information. As proved by the increase of the water signals at $3400\text{--}3600$ and 1630 cm^{-1} , passing from the totally dehydrated matrix (orange spectrum) to the fully hydrated system (blue spectrum), it is evident that the matrix is able to adsorb small amounts of water. However, the matrix-water affinity is certainly negligible, as demonstrated by the small amount of residual water present in the spectrum collected after a room temperature outgassing of just few seconds (see black dotted curve).

In a second moment, we investigated the interaction of SSD with water vapors. Figure 5 shows the FT-IR (parts a and c) and Raman (part b) spectra of the plain matrix (light grey), of anhydrous SSD (red) and of the same system in interaction with water vapors (violet). After contact with water, the Raman spectrum of SSD (Figure 5b) is greatly simplified. In particular, in the region of ν_1 vibrational mode of $[\text{ClO}_4]^-$ groups, a single absorption band is observed at 930 cm^{-1} , overlapped to the vibrational modes of the matrix.

In other words, the Raman spectrum of hydrated SSD is very similar to the sum of the spectra of the matrix and of hydrated $\text{Mg}(\text{ClO}_4)_2$ salt. This means that the $[\text{ClO}_4]^-$ groups in fully hydrated SSD exhibit the perfect tetrahedral symmetry typical of free perchlorate anions.

FT-IR spectroscopy allowed monitoring the interaction of SSD with increasing amount of water. The progressive hydration of SSD is testified by the growth of intense absorption bands in the ν_{OH} ($3700\text{-}3100\text{ cm}^{-1}$) and δ_{HOH} ($\sim 1650\text{-}1600\text{ cm}^{-1}$) regions (Figure 5a), in agreement with the high hydrophilic character of the composite. Simultaneously, the absorption bands characteristic of the highly dispersed anhydrous $\text{Mg}(\text{ClO}_4)_2$ salt (centered around 300 cm^{-1}) gradually shift at lower frequency (Figure 5c).

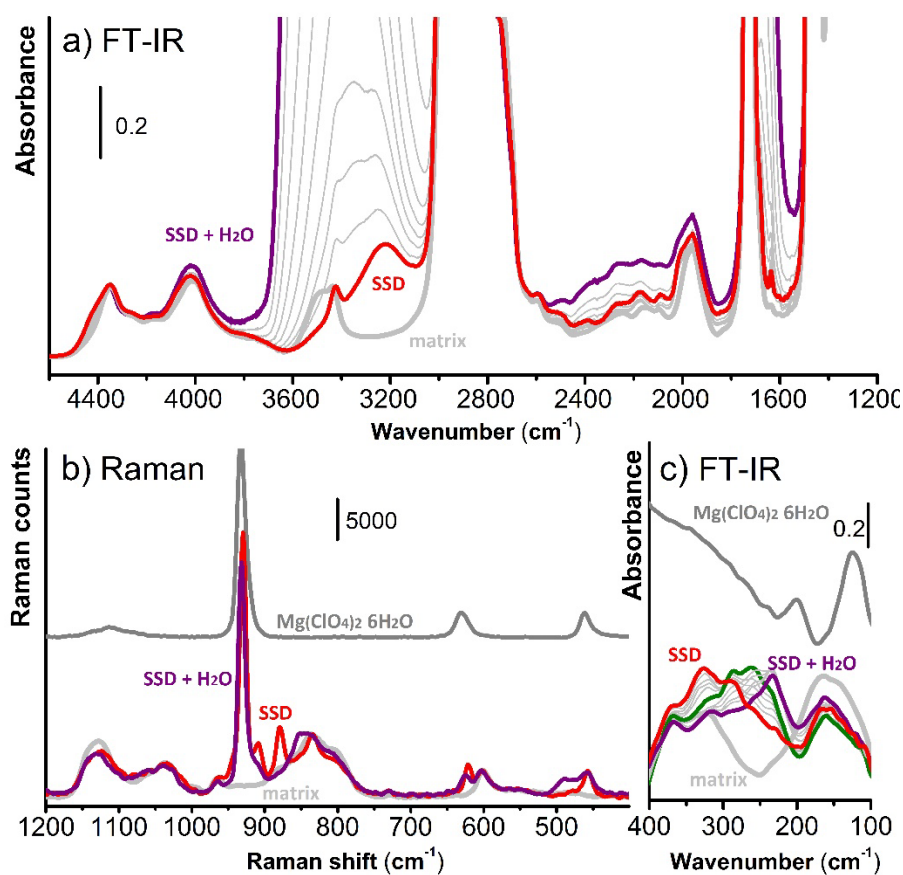


Figure 5. FT-IR (parts a and c) and Raman ($\lambda = 514$ nm, part b) spectra of $\text{Mg}(\text{ClO}_4)_2 \cdot 6\text{H}_2\text{O}$ (gray, vertically translated), of the polymeric matrix (light grey), of dehydrated SSD (red) and of fully hydrated SSD (violet). In parts a and c the spectra collected at intermediate hydration steps (from 0.1 mbar to water vapor pressure) are shown also (thin grey). Green spectrum in part c highlights an intermediate hydration step characterized by peculiar vibrational properties.

The evolution of the spectra occurs in two main steps: (i) at first, new IR absorption bands centered at around 250 cm^{-1} appear (green); the presence of an isosbestic point at 297 cm^{-1} testifies that the species responsible of the IR bands around 300 cm^{-1} in anhydrous SSD are transformed into new intermediate species; (ii) secondly, the intermediate spectrum (green) further evolves to give a final spectrum (violet) characterized by a main IR absorption band at 220 cm^{-1} ; a second isosbestic point is observed at 243 cm^{-1} . The absorption band centered at 220 cm^{-1} is very close to that observed in the spectrum of hexa-hydrated $\text{Mg}(\text{ClO}_4)_2$ (gray) and assigned to $\text{Mg}-\text{O}_{\text{H}_2\text{O}}$ stretching vibrations of Mg^{2+} cations completely surrounded by H_2O molecules. Hence, FT-IR data demonstrate that in

fully hydrated SSD the Mg^{2+} cations are completely solvated by the water molecules, in good agreement with Raman results.

Finally, at high wavenumbers (Figure 5a), the shoulder at 4430 cm^{-1} , previously indicated as an evidence of interaction between anhydrous $\text{Mg}(\text{ClO}_4)_2$ and the matrix, gradually disappear upon hydration of SSD. The FT-IR spectrum of fully hydrated SSD is coincident with that of the matrix in this spectral region, demonstrating that in the hydrated SSD the polymeric matrix is no longer perturbed by the presence of the dispersed salt.

Taken all together, the experimental results discussed above provide an evidence that the interactions at the molecular level established between anhydrous $\text{Mg}(\text{ClO}_4)_2$ and the polymeric matrix are no longer present in hydrated SSD, being the Mg^{2+} cations solvated by water. In the fully hydrated condition, the vibrational properties of SSD are coincident with the pure sum of the two constituents, *i.e.* the matrix and the exa-hydrated $\text{Mg}(\text{ClO}_4)_2$ salt.

4. Conclusions

We have investigated the functional properties of a new $\text{Mg}(\text{ClO}_4)_2$ -based polymeric composite material with water vapor getter properties. The composite system (SSD) is constituted by a $\text{Mg}(\text{ClO}_4)_2$ salt and a polymeric acrylic matrix; the salt is highly dispersed in the matrix, as demonstrated by XRPD data. The synergic combination of FT-IR and Raman spectroscopy allowed us to obtain additional information about the interactions occurring at the molecular level between the two constituents, which are at the basis of the function of SSD. It was found that in the anhydrous SSD composite the dispersed $\text{Mg}(\text{ClO}_4)_2$ salt retains its molecular structure, *i.e.* the Mg^{2+} cations are still surrounded by their $[\text{ClO}_4]^-$ counter-anions, and at the same time the salt and the polymeric matrix interact each other at the molecular level. These interactions gradually vanish in presence of water moisture, up to disappear in the fully hydrated SSD composite, because the Mg^{2+} cations are completely solvated by the water molecules.

These results highlight the role of interactions at the molecular level in determining the functional properties of composite materials originated from the combination of constituents having very different chemical nature. In addition, the important role of vibrational spectroscopy in the detailed characterization and optimization of these class of materials clearly emerges.

References

- 1) P.E. Burrows, V. Bulovic, S.R. Forrest, L.S. Sapochak, D.M. McCarty, M.E. Thompson. Reliability and Degradation of Organic Light Emitting Devices. *Appl. Phys. Lett.* 1994. 65 (23): 2922-2924.
- (2) S. Gardonio, L. Gregoratti, P. Melpignano, L. Aballe, V. Biondo, R. Zamboni, M. Murgia, S. Caria, M. Kiskinova. Degradation of organic light-emitting diodes under different environment at high drive conditions. *Org. Electron.* 2007. 8 (I): 37-43.
- (3) V. Bugatti, S. Concilio, P. Iannelli, S. Bellone, M. Ferrara, H.C. Neitzert, A. Rubino, D. Della Sala, P. Vacca. Synthesis and characterization of new electroluminescent molecules containing carbazole and oxadiazole units. *Synth. Met.* 2006. 156: 13–20.
- (4) P. Vacca, Dispensable polymeric precursor composition for transparent composite sorber materials. *PCT* 2012, WO045557A1.
- (5) H. K. Lim, Y. S. Choi, S. T. Hong. Magnesium perchlorate anhydrate, $Mg(ClO_4)_2$, from laboratory X-ray powder data. *Acta Crystallogr., Sect. C.* 2011. C67: i36-i38.
- (6) K. Robertson, D. Bish. Determination of the crystal structure of magnesium perchlorate hydrates by X-ray powder diffraction and the charge-flipping method. *Acta Crystallogr., Sect. B.* 2010. 66: 579-584.
- (7) D. R. Lide. *Handbook of Chemistry and Physics* 84th ed. Ohio: CRC Press. 2003-2004, 350.
- (8) H. H. Willard, G. F. Smith. The preparation and properties of magnesium perchlorate and its use as a drying agent. *J. Am. Chem. Soc.* 1922. 44: 2255-2259.

- (9) M. Chabanel, D. Legoff, K. Touaj. Aggregation of perchlorates in aprotic donor solvents. Part 1. Lithium and sodium perchlorates. *J. Chem. Soc., Faraday Trans.* 1996. 92: 4199-4205.
- (10) Y. Chen, Y. H. Zhang, L. J. Zhao. ATR-FT-IR spectroscopic studies on aqueous LiClO_4 , NaClO_4 , and $\text{Mg}(\text{ClO}_4)_2$ solutions. *Phys. Chem. Chem. Phys.* 2004. 6: 537-542.
- (11) B. J. Hathaway, A. Underhill. The infrared spectra of some transition-metal perchlorates. *J. Chem. Soc.* 1961. 6: 3091-3096.
- (12) F. A. Miller, C. H. Wilkins. Infrared Spectra and Characteristic Frequencies of Inorganic Ions. *Anal. Chem.* 1952. 24: 1253-1294.
- (13) J. L. Pascal, J. Potier, D. J. Jones, J. Roziere, A. Michalowicz. Structural approach to the behavior of perchlorate as a ligand in transition-metal complexes using EXAFS, IR, and Raman spectroscopy. 2. Crystal structure of $\text{M}(\text{ClO}_4)_2$ ($\text{M} = \text{Co}, \text{Ni}$). A novel mode of perchlorate coordination. *Inorg. Chem.* 1985. 24: 238-241.
- (14) J. L. Pascal, F. Favier. Inorganic perchlorato complexes. *Coord. Chem. Rev.* 1998. 178-180 (Part I): 865-902.
- (15) D. Cvjeticanin, S. Mentus, Conductivity, viscosity and IR spectra of Li, Na and Mg perchlorate solutions in propylene carbonate/water mixed solvents. *Phys. Chem. Chem. Phys.* 1999. 1: 5157-5161.
- (16) J. Mink, C. Nemeth, L. Hajba, M. Sandstrom, P. L. Goggin, Infrared and Raman spectroscopic and theoretical studies of hexaaqua metal ions in aqueous solution. *J. Mol. Struct.* 2003. 661-662: 141-151.